

## The Skin Effect in High Pressure Die Casting Al Alloys

Kun Vanna Yang, Anumalasetty Venkata Nagasekhar<sup>†</sup>,  
Roger Lumley<sup>1</sup>, Carlos Horacio Caceres<sup>\*</sup>

ARC CoE for Design in Light Metals, Materials Engineering,  
The University of Queensland, Brisbane, QLD-4072, Australia

<sup>1</sup>CSIRO Light Metals Flagship, Private bag 33, Clayton South MDC, Australia

\*c.caceres@uq.edu.au

Vickers microhardness cross sectional maps of cast-to-shape flat specimens 3 mm thick were determined for the (mass %) Al-9Si-2Cu-0.3Mg and Al-5Mg-2Si-Mn high pressure die cast alloys. Higher hardness numbers were generally obtained near the casting surface, the corner of the cross section and at the segregation band; they appeared connected with a locally finer grain size, the concentration of positive macro segregation and in some cases large intermetallic particles. Lower hardness numbers were found at the core and some stochastically distributed areas, which were accounted for by the locally coarser solidification microstructure and localized microporosity. The core region was up to some 15 HV softer than the surface layer. The maps indicated that the harder surface layer or skin was generally uneven and asymmetrical. The overall behavior of the microhardness was accounted for in terms of microporosity, grain size and intermetallic phases' distribution and uniformity in size.

**Keywords:** High pressure die casting; Aluminium alloys; Mechanical properties; Skin effect; Microhardness mapping.

### 1. Introduction

The good thermal contact between the die wall and the solidifying metal ensured by the applied pressure during solidification in high pressure die cast (HPDC) alloys [1-5] results in very high cooling rates, creating a very fine microstructure near the casting surface. In addition, the presence of externally solidified  $\alpha$  grains (ESG's) formed due to the premature solidification in the shot sleeve and runner, results in a bimodal grain size distribution, especially at the core region. The surface layer normally shows higher integrity, higher hardness and yield strength than the center or core region of the casting cross section, and is often referred to as the casting "skin". The enhanced properties of the skin region have been ascribed to a combination of very fine primary grains, significantly higher volume fraction of intermetallics and increased local supersaturation of solute in solution [1].

This work has been carried out to characterize the skin effect on HPDC Al-based alloys and to assess the similarities and differences in the microstructure and hardness profiles in relation to HPDC Mg-Al alloys [6, 7].

### 2. Materials and experimental details

Two Al based HPDC alloys were selected for this work: a Cu-containing alloy with nominal composition (mass %) Al-9Si-2Cu-0.3Mg from a prior study [8] and a high Mg alloy (Magsimal 59), with nominal composition Al-5Mg-2Si-Mn. These alloys represent widely different alloy families: the Magsimal 59 is strengthened largely by solid solution effects due to its high content of

---

<sup>†</sup> Current address: Carpenter Technology Corporation, P.O. Box 14662, Reading, PA 19612-4662, USA.

Mg whereas the Cu-containing alloy, with a much larger proportion of eutectic Si particles, has a somewhat lower yield strength but exhibits significantly more strain hardening.

Dog-bone shaped tensile specimens with rectangular cross section (5.75 mm width and 3 mm thickness) and gauge length 33 mm were cast to shape using a 250 t Toshiba cold chamber HPDC machine. As-cast specimens were used for the study.

Samples for microhardness testing and microstructural characterization were sectioned from the centre of tensile specimens and polished down to 0.05  $\mu\text{m}$  colloidal silica. An automated Vickers microhardness tester was used for the mapping, with a load of 50 gmf and a dwell time of 12 s. A minimum distance of 120  $\mu\text{m}$  away from the free surface or between adjacent indentations was set in accord with the ASTM E384-07 standard, by which at least 2.5 times the indentation diagonal (predetermined to be 30~40  $\mu\text{m}$ ) must separate adjacent indentations. The mapping was designed to cover the entire cross section of the samples. The coordinates of the indentation points and hardness numbers were profiled into a 3D hardness surface map using a commercial software package (Surfer). The microstructure was studied on sections adjacent to those used for the microhardness testing. Tensile testing was carried out on a hard beam machine, with double extensometers attached, at an extension rate of 1 mm/min.

### 3. Results

#### 3.1 Mechanical properties

##### *Tensile behaviour*

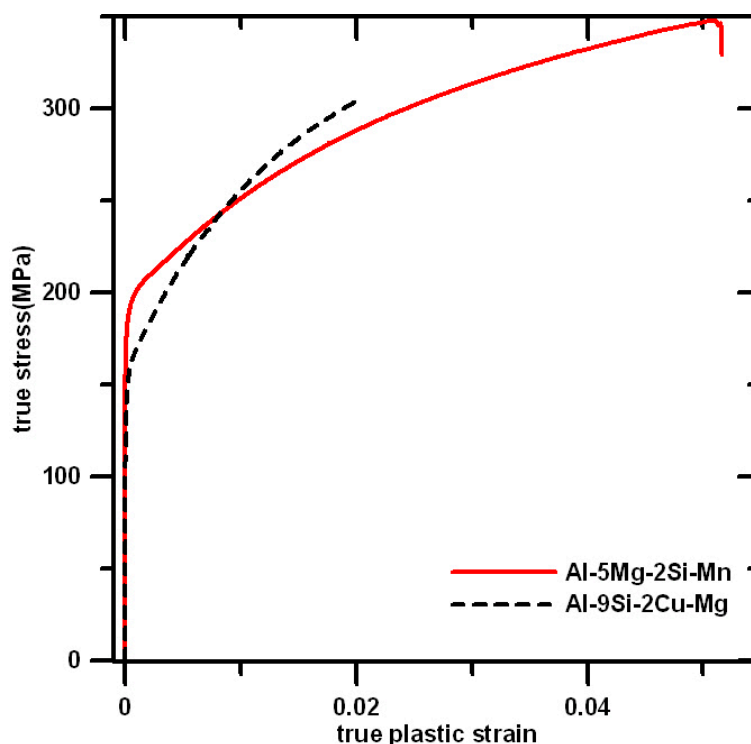


Fig. 1 True stress-true plastic strain curves for the alloys studied

Figure 1 compares the flow behaviour of the two alloys. Higher yield strength was observed for the Magsimal 59 alloy, at 209 MPa, compared to 183 MPa for the Al-9Si-2Cu-Mg alloy. The flow curves crossed each other at a plastic strain of about 0.007 due to the higher strain hardening rate exhibited by the Cu-containing alloy.

### Microhardness mapping

Figure 2 shows 3D microhardness maps of the specimens studied, together with their indentation patterns. A color scale is used to facilitate the comparison. The regions near the surface were harder than those at the center or core of the casting for both alloys. The hardness map of the Al-9Si-2Cu-Mg alloy, Fig. 2-a, exhibited many localized high hardness values, within the range 130-150 HV. Values above 110 HV in the periphery of the section roughly identified the “skin” region for this alloy. A softer core region, with a localized area of very low values, was also apparent in the map. The hardness value at the core varied between 50 and 90 HV.

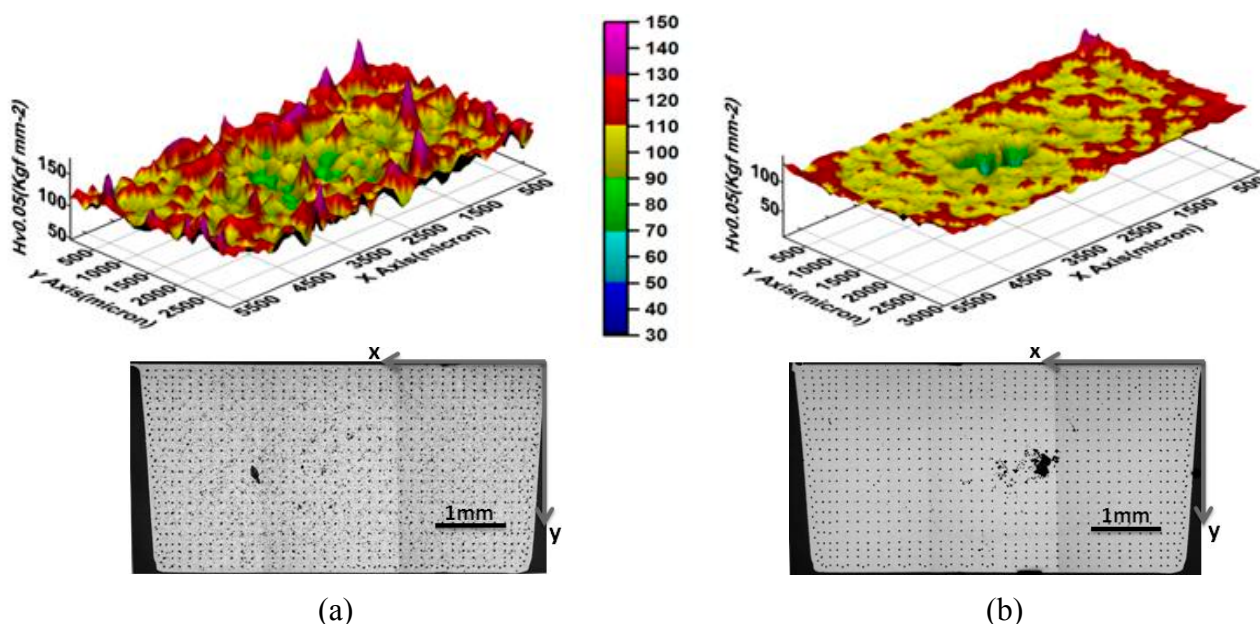


Fig. 2 Microhardness maps for the alloys investigated (a) Al-9Si-2Cu-Mg, (b) Al-5Mg-2Si-Mn together with a color scale and the indentation patterns.

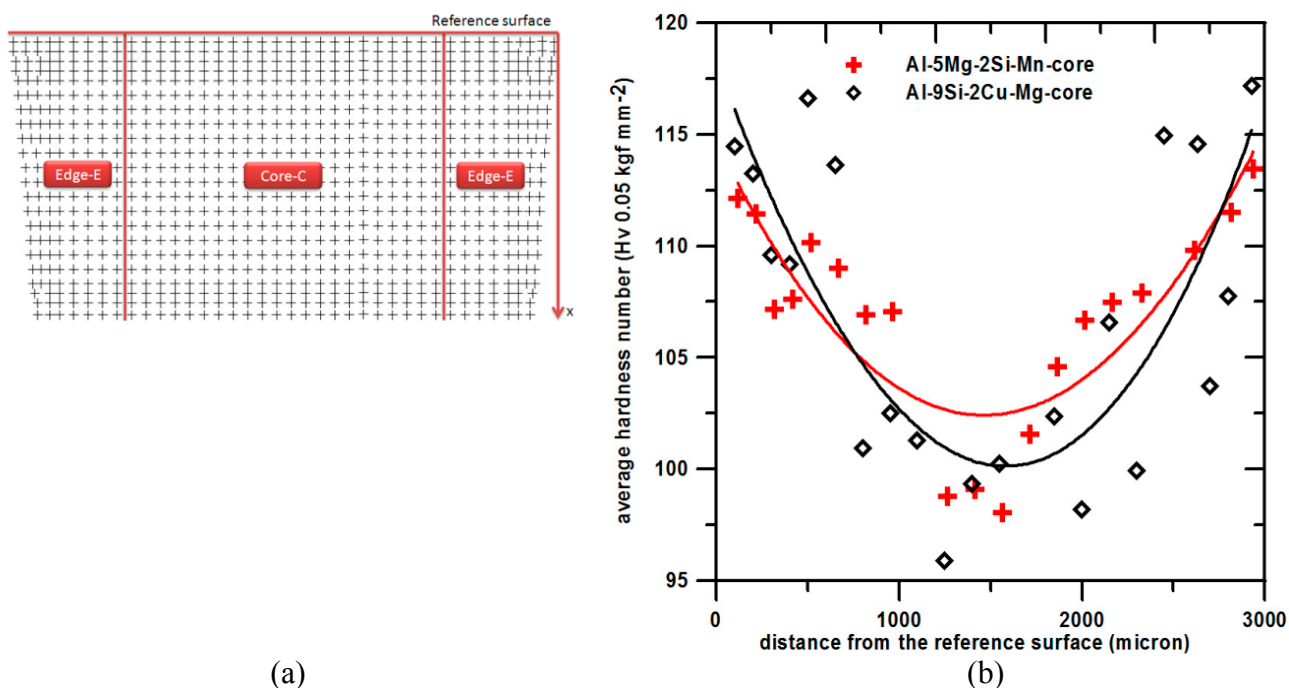


Fig. 3 (a) Indentation pattern showing the narrow edge and the core regions of the cross section; (b) The average hardness number across the thickness for the core region.

The hardness map for the Magsimal 59 alloy, shown in Fig. 2-b, was comparatively much smoother, with very few peaks above 130 HV. Somewhat higher hardness values, ranging from 110 to 130 HV were observed distributed along the periphery, but a distinct skin region was evident only in parts of the section. A few very low hardness number points, in the range 30~45 HV, were also found in the core region, due to localized shrinkage and gas porosity. At 104.4 HV, the average hardness of the entire Magsimal 59 cross section was slightly higher than that of the Cu-containing alloy, at 102.5 HV.

Fig. 3-a identifies the core and narrow edge regions of the sections, whereas Fig. 3-b shows the average hardness profile of the core regions. Both alloys exhibited a U-shaped hardness profile, with a difference between center and surface of about 15 HV.

### 3.2 Microstructural characterization

Figure 4 shows photomicrographs of the two alloys investigated. The images represent the corner, the surface at the middle of the long edge and the core of the cross section.

For the Al-9Si-2Cu-Mg, the microstructure consisted of primary  $\alpha$  (Al) phase, Al-Si eutectic, some Cu-bearing phases, and large Al-Si-Fe-Mn intermetallic particles, the latter identified by arrows in Fig. 3-a [8]. For the Al-5Mg-2Si-Mn, the microstructure consisted of  $\alpha$  (Al) phase, a network of eutectic particles, presumably eutectic  $Mg_2Si$ , and a dispersion of  $\pi$ - $Al_8FeMg_3Si_5$  and  $\beta$ - $Al_5FeSi$  particles [9].

The lowest concentration of externally solidified dendritic grains (ESG's) was found at the corner regions, followed by the surfaces, whereas the ESG's were prevalent at the core; the primary  $\alpha$  (Al) grain size was very small at the corner and the surface, but was somewhat larger at the core, in both alloys.

## 4. Discussion

Figure 4 shows that for both alloys the ESG's are much larger than the primary  $\alpha$  (Al) grains formed in the die cavity [10], and tended to concentrate at the core, therefore the locally larger average grain size. In addition, the ESG's have a lower content of solute in solution [11]. Thus, a lower amount of hardening due to grain size and a reduced solid solution content is expected at the core region, accounting for its lower hardness in the maps of Fig. 2 and the U-shaped profiles of Fig. 3.

Previous work on the Cu-containing alloy indicates that yield strength,  $\sigma_y$ , and hardness follow the relationship [8]:

$$\sigma_y(MPa) = 1.9HV - 18.8 \quad (1)$$

Assuming the Eq. (1) is valid for both alloys, a difference of 15 HV in hardness between surface and core represents approximately 28.5 MPa difference in yield strength, suggesting that the core is likely to yield first under load, whereas the skin would remain elastic.

The randomly distributed Al-Si-Fe-Mn intermetallic particles in the Al-9Si-2Cu-Mg alloy explained the localized peaks in hardness in Fig. 2-a, whereas the presence of microporosity caused the very low hardness points in Fig. 2-b. Stochastically distributed ESG's near the casting surface (Fig. 4) created local non uniformities in the grain microstructure, which accounted for localized variations in hardness aside from the peaks associated with large intermetallic particles. Overall, the results showed that the skin was generally uneven, non continuous and asymmetric for both alloys, in correlation with the lack of uniformity of the grain microstructure caused by the scattered distribution of ESG's. The lack of large Fe-rich intermetallic particles made the Magsimal 59's map much smoother.

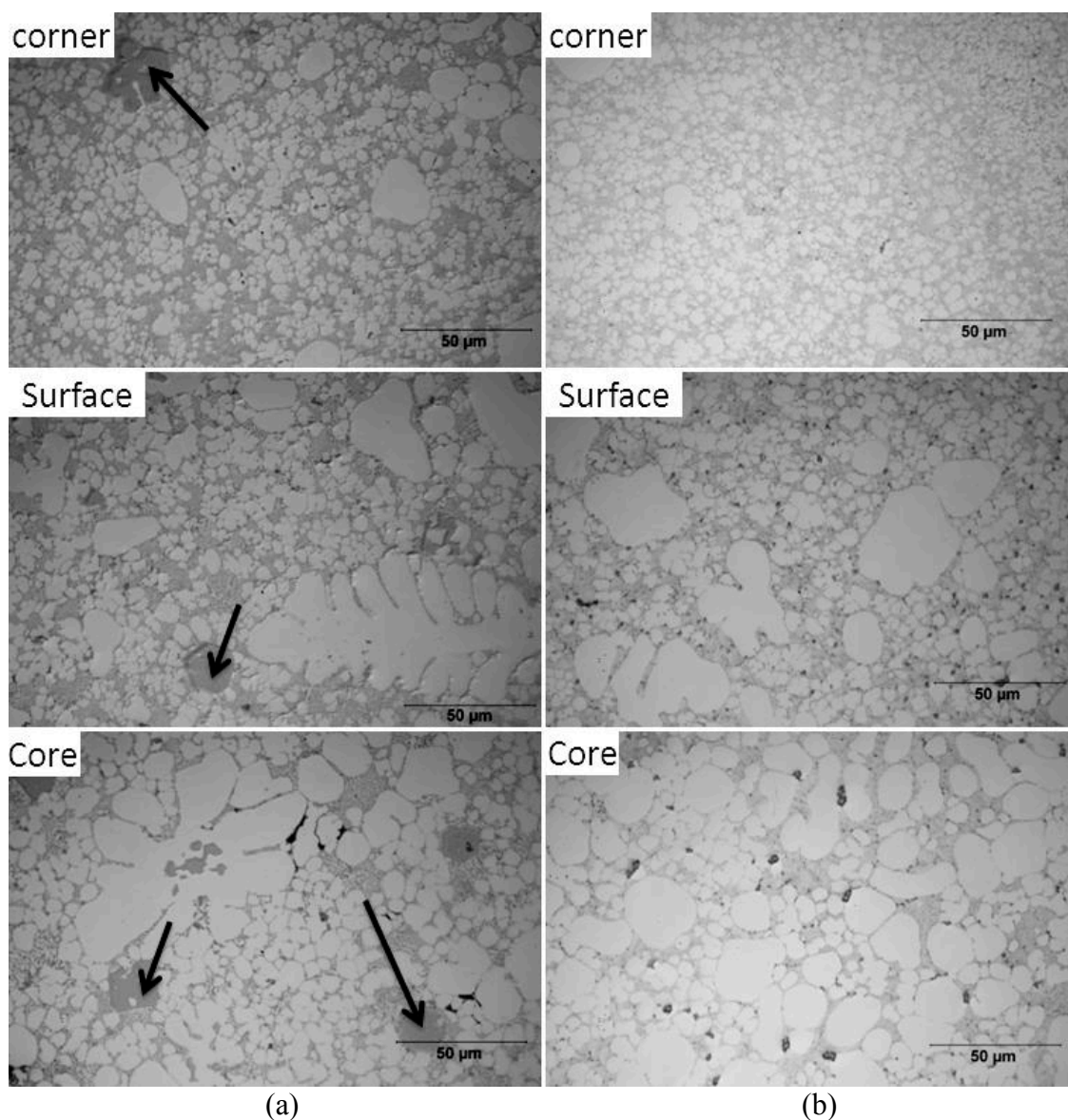


Fig. 4 Optical micrographs of different locations on the cross section (a) Al-9Si-2Cu-Mg, (b) Al-5Mg-2Si-Mn. The arrows identify the large Al-Si-Fe-Mn intermetallic particles in the Cu-containing alloy.

The average hardness values of the entire cross sections were quite similar to each other ( $HV = 104.4$  and  $HV = 102.5$ ) despite the difference in yield strength of about 26 MPa shown by Fig. 1. This can be easily rationalized by keeping in mind that hardness represents the strength of the material at some small strain [12]. Fig. 1 shows that the strain hardening rate of the Cu-containing alloy was significantly higher than that of the Magsimal 59, thus reducing the difference in yield strength as measured by hardness.

The hardness behavior of the Al based HPDC alloys mimicked that of Mg-Al based HPDC alloys described in [6, 13]. The microstructural features shown in Fig. 4 were also quite similar to those of the Mg-based alloys in terms of the bimodal grain size distribution caused by the scattered presence of ESG's and the finer primary grains near the casting surface. However, the presence of a distinct skin was less evident in the microhardness maps of the Al based alloys. This can be understood considering the much lower Hall-Petch strength coefficient,  $k$ , of Al alloys ( $k \sim 0.06$  MPa

$m^{1/2}$ ) [14] in comparison with that of Mg-Al alloys ( $k \sim 0.3 \text{ MPa m}^{1/2}$ ) [15], which thus limits the strengthening effect of the finer grain size near the casting surface of the Al alloys.

## 5. Summary

The hardness of HPDC Al-9Si-2Cu-Mg and Al-5Mg-2Si-Mn alloys was generally higher near the surface than at the core of the castings cross section. This behavior was accounted for by the finer grain structure near the surface or at the corners, and the coarser solidification microstructure and the concentration of porosity at the core. The randomly scattered distribution of externally solidified grains created a locally non uniform grain structure near the surface, leading to a non uniform and asymmetric skin over the entire cross-section. The overall skin effect was less evident in the hardness maps of the Al alloys than in Mg-based alloys, presumably due to the smaller Hall-Petch coefficient of the Al alloys.

## References

- [1] W.P. Sequeira, M.T. Murray, G.L. Dunlop, and D.H. StJohn, in: *TMS Symposium on automotive alloys*, The Minerals Metals and Materials Society (TMS), Warrendale, PA, 1997, pp. 169-183.
- [2] J.P. Weiler, J.T. Wood, R.J. Classen, R. Berkmortel, and G. Wang: *Materials Science and Engineering A* 2006, vol. 419, pp. 297-305.
- [3] J. Song, S.-M. Xiong, M. Li, and J. Allison: *Materials Science and Engineering A* 2009, vol. 520, pp. 197-201.
- [4] G. Pettersen, R. Hoier, O. Lohne, and H. Westengen: *Materials Science and Engineering A* 1996, vol. 207A, pp. 115-120.
- [5] Z.W. Chen: *Materials Science and Engineering A* 2003, vol. 348, pp. 145-153.
- [6] K. Yang, A.V. Nagasekhar, C.H. Caceres, and M.A. Easton: *Magnesium Technology 2010 TMS (The Minerals, Metals & Materials Society)* Warrendale, PA 2010, pp. 391-394.
- [7] K. Yang, A.V. Nagasekhar, C.H. Caceres, and M.A. Easton: *Advanced Materials Research*, 2010, vol. 97-101, pp. 743-747.
- [8] R.N. Lumley, R.G. O'Donnell, and D.R. Gunasegaram: *Metallurgical science and technology* 2008, vol. 26, pp. 2-7.
- [9] B. Johannesson and C.H. Caceres: *Int. J. Cast Metals Res.* 2004, vol. 17, pp. 94-98.
- [10] A.V. Nagasekhar, M.A. Easton, and C.H. Caceres: *Advanced Engineering Materials* 2009, vol. 11, pp. 912-919.
- [11] M.A. Easton, H. Kaufmann, and W. Fragner: *Materials Science and Engineering A* 2006, vol. 420, pp. 135-143.
- [12] M.C. Shaw: *The science of hardness testing and its research applications*, ASM, Metals Park, OH 1973, pp. 1-15.
- [13] C.H. Cáceres, J.R. Griffiths, A.R. Pakdel, and C.J. Davidson: *Materials Science and Engineering A* 2005, vol. 402, pp. 258-268.
- [14] J.D. Embury: *Strengthening methods in crystals*, Elsevier, London 1972, pp. 331-402.
- [15] J.P. Weiler, J.T. Wood, and R.J. Classen: *Journal of Materials Science* 2005, vol. 40, pp. 5999-6005.